Optomechanical two-photon hopping

Enrico Russo,[1,*] Alberto Mercurio,[1] Fabio Mauceri,[1] Rosario Lo Franco,[2] Franco Nori,[3,4,5] Salvatore Savasta,[1,3] and Vincenzo Macrì[3,2,†]

[1]*Dipartimento di Scienze Matematiche e Informatiche, Scienze Fisiche e Scienze della Terra, Università di Messina, I-98166 Messina, Italy*
[2]*Dipartimento di Ingegneria, Università degli Studi di Palermo, Viale delle Scienze, 90128 Palermo, Italy*
[3]*Theoretical Quantum Physics Laboratory, RIKEN, Wako-shi, Saitama 351-0198, Japan*
[4]*RIKEN Center for Quantum Computing (RQC), Wako-shi, Saitama 351-0198, Japan*
[5]*Physics Department, University of Michigan, Ann Arbor, Michigan 48109-1040, USA*

(Received 20 September 2022; revised 15 February 2023; accepted 26 February 2023; published 31 March 2023)

The hopping mechanism plays a key role in collective phenomena emerging in many-body physics. The ability to create and control systems that display this feature is important for next generation quantum technologies. Here we study two cavities separated by a vibrating two-sided perfect mirror and show that, within currently available experimental parameters, this system displays photon-pair hopping between the two electromagnetic resonators. In particular, the two-photon hopping is not due to tunneling, but rather to higher-order resonant processes. Starting from the classical problem we quantize the system and show this purely quantum feature. This opens the possibility to investigate a new mechanism of photon-pair propagation in optomechanical lattices.

DOI: 10.1103/PhysRevResearch.5.013221

I. INTRODUCTION

The mastery of manipulating quantum mechanical systems by means of radiation pressure has opened the door to fundamental tests of quantum theory [1,2], to precision measurements [3–5], and to novel quantum technologies [6–8]. For instance, laser cooling techniques [9–11] allow us to observe quantized vibrational modes of macroscopic objects and even the possibility to reach their ground state [12–14]. This has paved the way to the realization of entangled macroscopic states and, in turn, new ways to process and store quantum information [15–18]. Notably, with these techniques optomechanical crystals [19–21] can be scaled to form optomechanical arrays where, using hopping mechanisms, applications for quantum information processing have been proposed [22,23].

Cavity optomechanics, in particular, lies at the crossroads of wide research lines that are currently under active investigation. In experiments [8,17,24,25], only radiation pressure effects have been considered, as the cavity frequencies far outweigh the mirror ones. On the other hand, ultra-high-frequency mechanical oscillators [26,27] coupled to microwave ones offer the potential to observe, for instance, dynamical Casimir effects [28–33]. The case of one such mirror interacting with a single cavity mode was first considered in Ref. [34], and this study was later extended to include an incoherent excitation of the mirror [35,36]. In the same setup, back-reaction and dissipation effects have also been studied [37,38]. Finally, the case of a cavity with two moving walls was addressed [39–41]; in this case, the cavity field mediates an effective interaction between the two mirrors leading to a phonon hopping.

A suitable platform to experimentally reproduce these predictions is circuit optomechanics. In fact, the addition of artificial atoms in a superconducting microwave setup strengthens the coupling with the mechanical resonator [27,42,43], and the introduction high-frequency mirrors makes it a very promising setup. A valuable alternative would be to use a quantum simulator [44,45] with two *LC* circuits playing the role of the cavities and a superconducting quantum interference device (SQUID) playing the role of the high-frequency vibrating mirror.

The availability of these experimental platforms led us to design a system that, under certain resonance conditions, allows for a simultaneous hopping of a photon pair. The system consists of two noninteracting electromagnetic resonators separated by a movable two-sided perfect mirror. The vibrational modes of the mirror act as a mediator between the two resonators, making the photon-pair hopping possible. Even though the vibrating mirror separates both cavities, at the classical level a cavity-cavity interaction is still activated unless one of the two cavities is empty (see Appendix A). This hopping mechanism has purely quantum mechanical features. In fact, it gets activated also when classically forbidden, e.g., in the absence of the field on one side of the cavity. The quantum vacuum is filled with virtual particles.

Our Hamiltonian, obtained by quantizing the classical problem, generalizes the results in Ref. [46]. It accounts also for generic equilibrium positions of the mirror even though, in

*enricorussoxvi@gmail.com
†vincenzo.macri@riken.jp

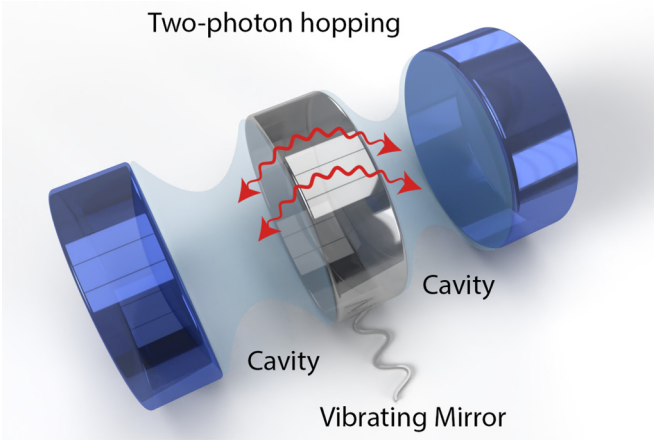

FIG. 1. Proposal sketch. Two noninteracting electromagnetic cavities separated by a movable two-sided perfect mirror.

what follows, we consider only the symmetric case. Similar setups have been studied, for instance, in Ref. [47], where the authors analyzed the dressing of the ground state and the correlation functions between the two separated regions, and in Ref. [48], where the two resonators are separated by a dielectric. In our treatment the two-photon hopping mechanism appears as a spontaneous coherent process in a second-order effective dynamics. Note that the optomechanical hopping described here does not involve photon tunneling, which is the usual photon hopping mechanism studied elsewhere [49–53].

Our interest in these hopping effects stems from the possibility to envision optomechanical lattices, with unit cells as in Fig. 1, and to study their thermodynamic and information properties. Thus, extended optomechanical lattices would display an interesting interplay between the Casimir photon-pair creation and the lattice intersite hopping.

In Sec. II, we give the quantum Hamiltonian for the system (see Appendix B), and provide an effective resonant description by applying the generalized James' method (see Appendix C). In Sec. III we report both analytical and numerical results for the dissipative system dynamics by using the Monte Carlo wave function approach (see Appendix D). The evolution of the wave function is studied, along one quantum trajectory and averaging over 500 quantum trajectories, by initializing the system with a Fock state. In a second simulation the evolution of the wave function is studied by initializing the system with a Gaussian coherent pulse. Finally, in Sec. IV, we give our conclusions.

II. THE QUANTUM MODEL

Consider two noninteracting electromagnetic cavities separated by a vibrating two-sided perfect mirror as sketched in Fig. 1. Following Ref. [46] we quantized (see Appendices A and B) the classical system obtaining the Hamiltonian ($\hbar = 1$)

$$\hat{H} = \omega_a \hat{a}^\dagger \hat{a} + \omega_b \hat{b}^\dagger \hat{b} + \omega_c \hat{c}^\dagger \hat{c} + \frac{g}{2}\left[(\hat{c}+\hat{c}^\dagger)^2 - \left(\frac{\omega_a}{\omega_c}\right)^2 (\hat{a}+\hat{a}^\dagger)^2\right](\hat{b}+\hat{b}^\dagger). \quad (1)$$

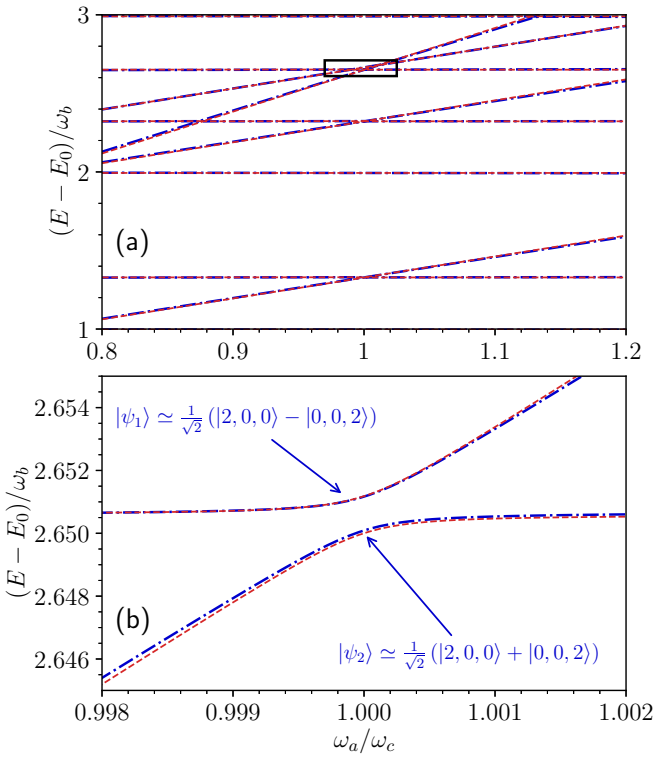

FIG. 2. (a) The lowest energy levels of the system Hamiltonian versus the ratio between the two cavity frequencies. For a coupling $g = 0.06\,\omega_b$, the position of the avoided-level crossing is contained in the black rectangular. (b) An enlarged view of the latter is given. The presence of the labels stresses the hybridization of the two states $|2,0,0\rangle$ and $|0,0,2\rangle$. The frequency mirror was conveniently set as $\omega_b = 3/4\,\omega_c$.

Here, $\hat{b}$ ($\hat{b}^\dagger$) is the creation (annihilation) operator of the moving mirror, and $\hat{a}$ ($\hat{a}^\dagger$) and $\hat{c}$ ($\hat{c}^\dagger$) are the creation (annihilation) operators of the left and right cavity, respectively. The parameters ω_a, ω_b, and ω_c are the corresponding bare energies of the three boson modes. The coupling strength $g = \omega_c^2\, x_{\rm zpf}/\pi = \omega_c\, x_{\rm zpf}/(I - q_0)$ (I and q_0 having the same units of $x_{\rm zpf}$, as reported in Appendix A) depends both on the zero-point-fluctuation amplitude of the mirror $x_{\rm zpf}$, and on the bare energy of a cavity ω_c, taken for convenience as the right one. The weight ω_a^2/ω_c^2 accounts for asymmetrical configurations. The linear approximation implicit in Eq. (1) does not lead to instabilities of the ground state as long as $g\omega_a < \omega_c^2$, i.e., $\omega_a x_{\rm zpf} < \pi$. The sought-after hopping mechanism occurs at the resonance $\omega_a = \omega_c$. We consider the case when the bare frequency of the mirror is lower than the cavity frequency. This choice of parameters identifies a set of avoided-level crossings in the Hamiltonian spectrum, and thus a particular closed subdynamics, as can be seen from Fig. 2. Indeed, Fig. 2(a) shows the lowest energy levels obtained by numerically diagonalizing the full Hamiltonian Eq. (1) (blue dash-dotted curves), while Fig. 2(b) is an enlarged view of the avoided-level crossing inside the black rectangle. The gap is a trademark of the hybridization of the two states $|\psi_1\rangle$ and $|\psi_2\rangle$, eigenstates of the full Hamiltonian Eq. (1). A local effective description (red dashed curves) is possible through the generalized James' effective approach [54] (see Appendix C), with

resonance conditions $\omega_c = \omega_a$:

$$\begin{aligned}\hat{H}^{(2)}_{\rm eff} &= \hat{H}^{(2)}_{\rm shift} + \hat{H}^{(2)}_{\rm hop},\\ \hat{H}^{(2)}_{\rm shift} &= \left[\omega_a + \frac{g^2(4\omega_a+\omega_b)}{8\omega_a^2-2\omega_b^2}\right](\hat{c}^\dagger\hat{c}+\hat{a}^\dagger\hat{a})\\ &\quad + \frac{g^2\left(3\omega_b^2-8\omega_a^2\right)}{\left(8\omega_a^2-2\omega_b^2\right)\omega_b}[(\hat{c}^\dagger\hat{c})^2+(\hat{a}^\dagger\hat{a})^2]\\ &\quad + \left[\omega_b + \frac{4g^2\omega_a}{4\omega_a^2-\omega_b^2}(\hat{a}^\dagger\hat{a}+\hat{c}^\dagger\hat{c}+\mathbb{1})\right]\hat{b}^\dagger\hat{b}\\ &\quad + \frac{2g^2}{\omega_b}\hat{a}^\dagger\hat{a}\hat{c}^\dagger\hat{c} + \frac{g^2}{2\omega_a-\omega_b}\mathbb{1},\\ \hat{H}^{(2)}_{\rm hop} &= -\frac{g^2\omega_b}{8\omega_a^2-2\omega_b^2}(\hat{a}^2\hat{c}^{\dagger 2}+\hat{a}^{\dagger 2}\hat{c}^2). \end{aligned} \tag{2}$$

The first term, $\hat{H}^{(2)}_{\rm shift}$, contains the bare Hamiltonians and both cross- and self-Kerr nonlinearities. The second term, $\hat{H}^{(2)}_{\rm hop}$, is the one responsible for the two-photon hopping. Since $[\hat{a}^\dagger\hat{a}, \hat{H}^{(2)}_{\rm shift}] = [\hat{b}^\dagger\hat{b}, \hat{H}^{(2)}_{\rm shift}] = [\hat{c}^\dagger\hat{c}, \hat{H}^{(2)}_{\rm shift}] = 0$ we can still choose as an unperturbed base the states $|n_a, n_b, n_c\rangle$, where n_a (n_c) is the number of photon in the left (right) cavity, and n_b the number of phonons in between; all of these three are considered with shifted energies due to interaction with the fields.

III. RESULTS

A. Analytical approach

The two states $|\psi_{1,2}\rangle = (|2,0,0\rangle \pm |0,0,2\rangle)/\sqrt{2}$ are eigenstates of the full (effective) Hamiltonian. To have a simple analytical description, we limit our analysis to the subspace spanned by $\{|2,0,0\rangle, |0,0,2\rangle\}$ around the avoided-level crossing. If we initialize the system in either $|2,0,0\rangle$ or $|0,0,2\rangle$, we witness a coherent oscillatory dynamics between the two maximally entangled photon-pair states. Neglecting dressing energy shifts, which have been reabsorbed by an appropriate choice of the coefficients, the effective interaction Hamiltonian $\hat{H}^{(2)}_{\rm hop}$ in Eq. (2) can be used to solve the stochastic evolution of the system wave function (see Appendix D). By projecting the time-evolution operator $\hat{U}(t) = \exp(-i\hat{\mathcal{H}}t)$ onto the $2D$ subspace $\{|2,0,0\rangle, |0,0,2\rangle\}$, with

$$\hat{\mathcal{H}} = \hat{H}^{(2)}_{\rm hop} - i(\gamma_a\hat{a}^\dagger\hat{a} + \gamma_b\hat{b}^\dagger\hat{b} + \gamma_c\hat{c}^\dagger\hat{c})/2, \tag{3}$$

in the interaction picture we obtain

$$\begin{aligned}\hat{U}(t) = e^{-2\gamma t}[&\cos(\tilde{g}t)(|2,0,0\rangle\langle 2,0,0| + |0,0,2\rangle\langle 0,0,2|)\\ &- i\sin(\tilde{g}t)(|2,0,0\rangle\langle 0,0,2| + |0,0,2\rangle\langle 2,0,0|)],\end{aligned} \tag{4}$$

where we choose $\gamma = \gamma_a = \gamma_c$ and $\tilde{g} = g^2\omega_b/2(4\omega_a^2 - \omega_b^2)$. If we initialize the system in the state $|2,0,0\rangle$, its evolution at time t, before a quantum jump takes place, is

$$|\psi(t)\rangle = e^{-2\gamma t}[\cos(\tilde{g}t)|2,0,0\rangle - i\sin(\tilde{g}t)|0,0,2\rangle]. \tag{5}$$

By appropriately renormalizing the wave function, we obtain the mean photon number for the left and right cavities and for the mechanical resonator:

$$\begin{aligned}\langle\hat{a}^\dagger\hat{a}\rangle &= 2\cos^2(\tilde{g}t),\\ \langle\hat{b}^\dagger\hat{b}\rangle &= 0,\\ \langle\hat{c}^\dagger\hat{c}\rangle &= 2\sin^2(\tilde{g}t).\end{aligned} \tag{6}$$

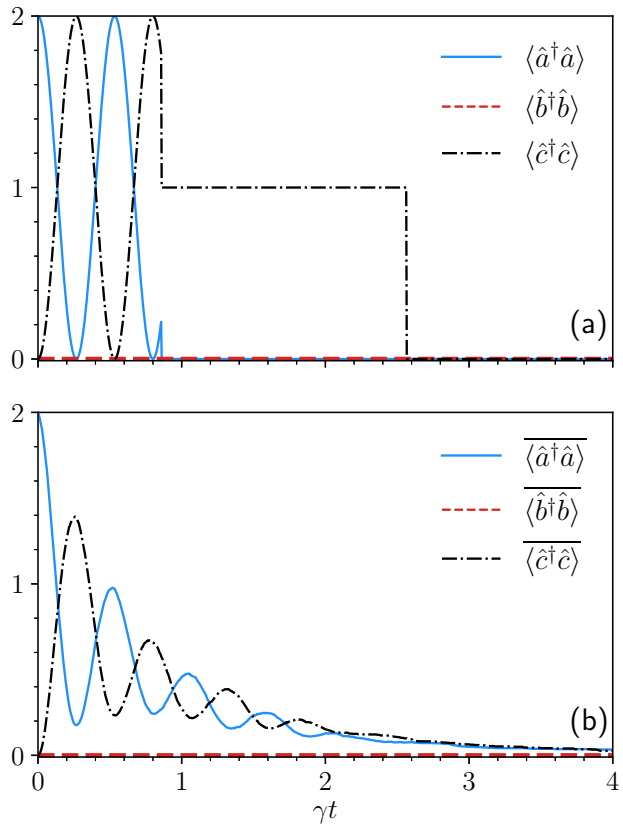

FIG. 3. Panel (a) shows an example of a single quantum trajectory, numerically obtained by studying the open quantum dynamics. It shows the time evolution of the mean photon number of the left cavity $\langle\hat{a}^\dagger\hat{a}\rangle$ (blue curve), right cavity $\langle\hat{c}^\dagger\hat{c}\rangle$ (black dash-dotted curve), and of the phonon number of the movable mirror $\langle\hat{b}^\dagger\hat{b}\rangle$ (red dashed curve). The system is initialized in $|2,0,0\rangle$ at the resonant condition $\omega_c = \omega_a$ and $\omega_b = 3\omega_a/4$. The numerical simulation initially displays the oscillation predicted by Eq. (5) until a quantum jump occurs in the right cavity. The measure collapses the state into $-i|0,0,1\rangle$. Even though the two cavities are in resonance, the state $|0,0,1\rangle$ is locked: the photon remains confined in the right cavity. This is an optomechanical feature of our system. After the second jump occurs, the system reaches the state $|0,0,0\rangle$. In panel (b) an average over 500 trajectories is shown. Clearly, there is a coherent evolution of two photon-pair states. Such results can be attained as well with a master equation approach, but the locking feature is lost in the average. In both panels, the parameters are $g = 0.06\,\omega_b$, $\omega_a = \omega_c = 4\omega_b/3$, and $\gamma_a = \gamma_b = \gamma_c = \gamma = 10^{-4}\omega_b$.

B. Numerical approach

1. Initial Fock state

We observe that Eq. (6) can be used to reproduce the numerical results shown in Fig. 3. The expectation value on a single quantum trajectory [see Fig. 3(a)] for a generic operator $\hat{O}$ is denoted as $\langle\hat{O}(t)\rangle$, while average quantities

obtained over an ideally infinite number of quantum trajectories [500 trajectories in the case of the Fig. 3(b)] are indicated as $\overline{\langle \hat{O}(t) \rangle}$. In particular, Fig. 3(a) shows an example of a single quantum trajectory, obtained by solving numerically the stochastic evolution of the system wave function. It shows the time evolution of the mean photon number $\langle \hat{a}^\dagger \hat{a} \rangle$ (blue curve) and $\langle \hat{c}^\dagger \hat{c} \rangle$ (black dash-dotted curve), of the left and right cavity, respectively, and the phonon number $\langle \hat{b}^\dagger \hat{b} \rangle$ (red dashed curve). The system is initialized in the state $|2, 0, 0\rangle$, as in the analytical case. Before a quantum jump occurs, the numerical simulation displays the oscillation predicted by Eq. (6). When the right detector clicks, one photon has escaped from the right cavity. Therefore, the state in Eq. (5) collapses to $-i|0, 0, 1\rangle = \hat{c}|\psi(t)\rangle/[\langle\psi(t)|\hat{c}^\dagger\hat{c}|\psi(t)\rangle]^{1/2}$. This state is preserved until a second jump occurs; i.e., the photon remains locked in the right cavity. This is an optomechanical feature of our system. Indeed, the absence of linear interaction terms in Eq. (2) denies a one-to-one conversion among the subsystems. Hence, when the second photon jump occurs, it is certain that the state collapses to $|0, 0, 0\rangle = \hat{c}|0, 0, 1\rangle$.

In Fig. 3(b) the dynamics is shown averaged over 500 trajectories. Clearly, we see a coherent oscillation of a photon pair. Of course, in the presence of decoherence, such result can be obtained also adopting a master equation approach, but the locking feature emerges only under a postselection procedure or by studying a single quantum trajectory [55,56]. Note that with the parameters used we obtain an effective coupling $\tilde{g} \approx 3 \times 10^{-4}\omega_b$, which is almost three times greater than the loss rate γ (the latter related to the cavity quality factor Q). This regime, defined as strong coupling, allows the photon pairs to flow from one cavity to the other for a certain time before one photon is lost to the environment.

2. *Driven by a Gaussian coherent pulse*

Finally, we consider the case of an incoming Gaussian coherent pulse driving the left cavity while the system is initially in its ground state. For simplicity we present a numerical simulation for the closed dynamics. Figure 4 shows the first matrix elements of the density operator at the end of the dynamics. The state of the right cavity contains only even occupation numbers: in a closed dynamics no loss is possible and the hopping mechanism always involves photon pairs.

IV. CONCLUSIONS

We have carried out a theoretical analysis of an optomechanical system consisting of two electromagnetic resonators separated by a vibrating two-sided perfect mirror. The Hamiltonian of the system is obtained starting from its canonical quantization, as shown in Appendices A and B, and it accounts also for generic equilibrium positions of the mirror. Our main result is the discovery of a photon-pair hopping mechanism, in a coherent second-order effective resonant dynamics.

This effect has been described analytically through the generalized James' approach (Appendix C) under the condition $\omega_a = \omega_c$. The numerical analysis of the lowest energy levels showed an avoided-level crossing around the resonant

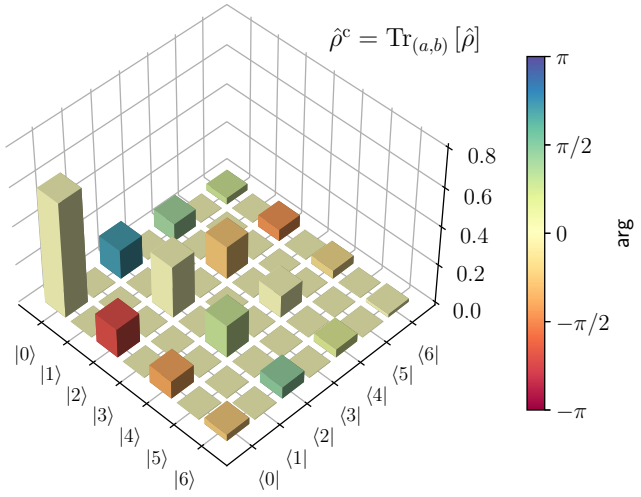

FIG. 4. Density matrix elements of the right cavity. It is obtained partially tracing over the left cavity and the mirror. Only *even-number states* are filled when the right cavity is initially empty and a coherent incoming pulse enters the left cavity. This is in full agreement with the hopping mechanism we proposed. The parameters used here are $g = 0.09\,\omega_b$, $\omega_a = \omega_c = 1.1\omega_b$, and $\gamma_a = \gamma_b = \gamma_c = 0$.

condition [see Fig. 2(c)]. This gap is a trademark of the hybridization of two photon-pair states. We have performed a stochastic evolution of the system wave function in which we witnessed a coherent oscillatory dynamics between the states $|2, 0, 0\rangle$ and $|0, 0, 2\rangle$.

The effects described here could be experimentally reproduced, with the chosen parameters, in circuit-optomechanical systems by using ultra-high-frequency mechanical micro- or nano-resonators in the GHz spectral range; alternatively, using two *LC* circuits bridged by a SQUID. Moreover, in arrays of nonlinearly coupled cavities [57], where the photon crystal associated to a periodic modulation of the photon blockade can emerge, the optomechanical system proposed here allows investigating a new mechanism of photon-pair propagation in optomechanical lattices [58,59].

ACKNOWLEDGMENTS

F.N. is supported in part by Nippon Telegraph and Telephone Corporation (NTTINK) Research, the Japan Science and Technology Agency (JST) [via the Quantum Leap Flagship Program (Q-LEAP) and the Moonshot R&D Grant No. JPMJMS2061], the Japan Society for the Promotion of Science (JSPS) [via the Grant-in-Aid for Scientific Research (KAKENHI) Grant No. JP20H00134], the Army Research Office (ARO) (Grant No. W911NF-18-1-0358), the Asian Office of Aerospace Research and Development (AOARD) (via Grant No. FA2386-20-1-4069), and the Foundational Questions Institute Fund (FQXi) via Grant No. FQXi-IAF19-06. S.S. acknowledges the Army Research Office (ARO) (Grant No. W911NF-19-1-0065). R.L.F. is supported by the European Union (Next Generation EU) via MUR D.M. Grant No. 737-2021.

APPENDIX A: DERIVATION OF THE CLASSICAL HAMILTONIAN

We begin by considering two noninteracting electromagnetic cavities separated by a perfect movable mirror. For simplicity, following Ref. [46], we conduct our analysis in $1D$ and generalize it to our case. To set the notation, $\pm I$ denotes the extremes of the cavity, M and $q(t)$ the mass and the position of the movable mirror, respectively. The electromagnetic field, in absence of charges, obeys the wave equation; the motion of the movable mirror is influenced by the radiation pressure of the fields in the two cavities [see Fig. 2(a) in the main text], so that it satisfies the Newton's equation ($c = 1$)

$$\begin{aligned} &\Delta A = 0, \qquad x \in (-I, q) \cup (q, I), \\ &M\ddot{q} = -\partial_q V + \tfrac{1}{2}[(\partial_- A)^2 - (\partial_+ A)^2]|_q, \end{aligned} \tag{A1}$$

where $\Delta := \partial_t^2 - \partial_x^2$ and ∂_-, ∂_+ are the left and right derivatives. The potential $V(q)$ is designed to have infinite walls at the two mirror positions $\pm I$. The two radiation pressures $(\partial_\pm A)^2/2$ come with opposite signs and in the form of lateral derivatives, because of the negligible thickness of the movable mirror.

By defining L_k and R_k as the Fourier components on the left and right cavity, respectively, the completeness of the mode functions enables us to write (from now on, we adopt the Einstein summation convention)

$$A(t, x) = \begin{cases} L^k(t)\,\varphi_k(t, x), & x \in (-I, q), \\ R^k(t)\,\phi_k(t, x), & x \in (q, I), \end{cases} \tag{A2}$$

where the summation in k is understood, and

$$\begin{aligned} \varphi_k &= \sqrt{\frac{2}{q+I}} \sin\left[\omega_k (x+I)\right], \\ \phi_k &= \sqrt{\frac{2}{I-q}} \sin\left[\Omega_k (x-I)\right], \end{aligned} \tag{A3}$$

with $\omega_k = k\pi/(q+I)$, $\Omega_k = k\pi/(I-q)$. We can still fix a normalization for φ_k and ϕ_k, choosing

$$\delta_{ij} = \int_{-I}^{q} \varphi_i \varphi_j = \int_{q}^{I} \phi_i \phi_j, \tag{A4}$$

as the Kronecker delta. The wave equation Eq. (A1) can be projected along one Fourier component, and the equation of motion of the movable mirror becomes

$$\begin{aligned} &\ddot{L}_k + \omega_k^2 L_k - \frac{g_{km}(2\dot{q}\dot{L}^m + \ddot{q}L^m)}{I+q} + \dot{q}^2 \frac{(g_{km} + g_{kj}g^j{}_m)L^m}{(I+q)^2} = 0, \\ &\ddot{R}_k + \Omega_k^2 R_k - \frac{\gamma_{km}(2\dot{q}\dot{R}^m + \ddot{q}R^m)}{I-q} - \dot{q}^2 \frac{(\gamma_{km} - \gamma_{kj}\gamma^j{}_m)R^m}{(I-q)^2} = 0, \\ &M\ddot{q} + \partial_q V + (-1)^{k+m}\left(\frac{\Omega_k \Omega_m R^k R^m}{I-q} - \frac{\omega_k \omega_m L^k L^m}{q+I}\right) = 0, \end{aligned} \tag{A5}$$

with

$$g_{km} = (q+I)\int_{-I}^{q} \partial_q(\varphi_k)\varphi_m = -\gamma_{km} = -(I-q)\int_{q}^{I} \partial_q(\phi_k)\phi_m, \tag{A6}$$

that satisfy

$$g_{kj}g^j{}_m = -(q+I)^2 \int_{-I}^{q} \partial_q\varphi_k \partial_q \varphi_m = \gamma_{kj}\gamma^j{}_m = -(I-q)^2 \int_{q}^{I} \partial_q\phi_k \partial_q \phi_m, \tag{A7}$$

and

$$\begin{aligned} \int_{-I}^{q} \varphi_k \partial_q^2 \varphi_m &= \frac{1}{(q+I)^2}\left(g_{kj}g^j{}_m - g_{km}\right), \\ \int_{q}^{I} \phi_k \partial_q^2 \phi_m &= \frac{1}{(I-q)^2}\left(\gamma_{kj}\gamma^j{}_m + \gamma_{km}\right). \end{aligned} \tag{A8}$$

The system of equations Eq. (A1) can be derived from the following Lagrangian,

$$\begin{aligned} \mathcal{L}(q, \dot{q}, L, \dot{L}, R, \dot{R}) = &\frac{1}{2}\left(\dot{L}_k\dot{L}^k - \omega_k^2 L_k L^k + \dot{R}_k\dot{R}^k - \Omega_k^2 R_k R^k\right) - \dot{q}\left(g_{km}\frac{\dot{L}^k L^m}{q+I} + \gamma_{km}\frac{\dot{R}^k R^m}{I-q}\right) \\ &- \frac{\dot{q}^2}{2}\left[g_{kj}g^j{}_m \frac{L^k L^m}{(q+I)^2} + \gamma_{kj}\gamma^j{}_m \frac{R^k R^m}{(I-q)^2}\right] + \frac{1}{2}M\dot{q}^2 - V, \end{aligned} \tag{A9}$$

and the corresponding Hamiltonian is

$$\mathcal{H}(q, p, L, \Lambda, R, W) = \frac{1}{2M}\left(p + g_{km}\frac{\Lambda^k L^m}{q+I} + \gamma_{km}\frac{W^k R^m}{I-q}\right)^2 + V + \frac{1}{2}\left(\Lambda_k\Lambda^k + \omega_k^2 L^k L^k\right) + \frac{1}{2}\left(W_k W^k + \Omega_k^2 R^k R^k\right). \tag{A10}$$

Before quantizing the classical Hamiltonian in Eq. (A10), let us consider the classical system of equations in Eq. (A5). The equations for L_k and R_k are homogeneous and the coefficients are nontrivial functions of $q, \dot{q}, \ddot{q}$; an initial condition $R_k(0) = \dot{R}_k(0) = 0$, representing the absence of the field on the right cavity side at the initial time, would be indeed satisfied by the trivial solution $R_k(t) = 0$ at all times. Since this is a well-posed Cauchy problem, the solution of the equation is unique and thus $R_k(t)$ remains identically zero no matter the values of L_k. Furthermore, if we consider the energy of the right electromagnetic field,

$$\begin{aligned}\mathcal{U} &= \frac{1}{2}\int_q^I [(\dot{A})^2 + (\partial_x A)^2]dx \\ &= \frac{1}{2}\left[\dot{R}^k\dot{R}_k - \frac{\dot{q}^2}{(I-q)^2}\gamma_{ki}\gamma^i_j R^k R^j\right], \end{aligned} \tag{A11}$$

by virtue of Eq. (A2), Eq. (A3), Eq. (A4), and Eq. (A7) (the sum over k, i, and j is understood). Clearly, this energy depends on the states of the mechanical mirrors allowed by the equations of motion. If the right cavity is empty, then the energy is constantly zero and the left electromagnetic field cannot be transferred to the right side. These properties reflect the perfection of the mirror and the fact that classical vacuum is empty.

APPENDIX B: QUANTIZATION OF THE CLASSICAL SYSTEM HAMILTONIAN

Consider the operators $\{\hat{q}, \hat{p}, \hat{L}_k, \hat{\Lambda}_k, \hat{R}_k, \hat{W}_k\}$ and impose the commutation relations ($\hbar = 1$) $[\hat{q}, \hat{p}] = i$, $[\hat{L}_k, \hat{\Lambda}_m] = i\delta_{km}$, and $[\hat{R}_k, \hat{W}_m] = i\delta_{km}$, while $[\hat{q}, \hat{L}_m] = [\hat{q}, \hat{R}_m] = [\hat{L}_k, \hat{R}_m] = [\hat{p}, \hat{L}_m] = [\hat{p}, \hat{W}_m] = [\hat{\Lambda}_k, \hat{W}_m] = 0$. Using the ladder operators,

$$\begin{aligned}\hat{a}_k &= \frac{1}{\sqrt{2\omega_k}}(\omega_k\hat{L}_k + i\hat{\Lambda}_k), \\ \hat{c}_k &= \frac{1}{\sqrt{2\Omega_k}}(\Omega_k\hat{R}_k + i\hat{W}_k), \end{aligned} \tag{B1}$$

the Hamiltonian Eq. (A10) becomes

$$\begin{aligned}\hat{H}' = &\frac{(\hat{p}+\hat{\Gamma})^2}{2M} + \hat{V} + \sum_k \omega_k\hat{a}^\dagger_k\hat{a}_k \\ &+ \sum_k \Omega_k\hat{c}^\dagger_k\hat{c}_k - \frac{\pi q\hat{\mathbb{1}}}{6(q+I)(q-I)}, \end{aligned} \tag{B2}$$

where we have already resummed the vacuum point fluctuations, and

$$\begin{aligned}\hat{\Gamma} = \frac{i}{2}\sqrt{\frac{m}{k}}\Bigg[&\frac{g^{km}(\hat{a}^\dagger_k - \hat{a}_k)(\hat{a}^\dagger_m + \hat{a}_m)}{q+I} \\ &+ \frac{\gamma^{km}(\hat{c}^\dagger_k - \hat{c}_k)(\hat{c}^\dagger_m + \hat{c}_m)}{I-q}\Bigg]. \end{aligned} \tag{B3}$$

This is the full Hamiltonian of the problem. To obtain Eq. (1) in the main text we need to linearize it and consider the unimodal case. To linearize, first consider $\Gamma \approx \Gamma_0$ constant and then introduce a variation from the expected position of the mirror $q = q_0 + \delta q$, and expand all the terms accordingly,

$$\begin{aligned}\omega_k &= \frac{k\pi}{q_0+I}\left(1 - \frac{\delta q}{q_0+I}\right) + \mathcal{O}\left[\frac{\delta q^2}{(q_0+I)^2}\right], \\ \Omega_k &= \frac{k\pi}{I-q_0}\left(1 + \frac{\delta q}{I-q_0}\right) + \mathcal{O}\left[\frac{\delta q^2}{(I-q_0)^2}\right], \end{aligned} \tag{B4}$$

which in turn, from Eq. (B1), induces

$$\begin{aligned}\hat{a}_k &\approx (\hat{a}_0)_k - \frac{\delta q}{2(q_0+I)}(\hat{a}^\dagger_0)_k, \\ \hat{c}_k &\approx (\hat{c}_0)_k + \frac{\delta q}{2(I-q_0)}(\hat{c}^\dagger_0)_k. \end{aligned} \tag{B5}$$

Performing the unitary transformation $\hat{U} = \exp(i\delta q\hat{\Gamma}_0)$ on Eq. (B2) proves that

$$\begin{aligned}\hat{H} = \hat{U}\hat{H}'\hat{U}^\dagger = &\frac{\hat{p}^2}{2M} + \hat{\mathcal{V}} + \sum_k[(\omega_0)_k(\hat{a}^\dagger_0)_k(\hat{a}_0)_k \\ &+ (\Omega_0)_k(\hat{c}^\dagger_0)_k(\hat{c}_0)_k] - \delta q(\hat{G}_0 + \hat{F}_0), \end{aligned} \tag{B6}$$

where $\hat{\mathcal{V}} = \hat{V} - \pi q\hat{\mathbb{1}}/6(q+I)(q-I)$ and

$$\begin{aligned}\hat{F}_0 &= \sum_{k,j}\frac{(-1)^{k+j}}{2(q_0+I)}\sqrt{(\omega_k\omega_j)_0}\,(\hat{a}^\dagger_k + \hat{a}_k)(\hat{a}^\dagger_j + \hat{a}_j), \\ \hat{G}_0 &= \sum_{k,j}\frac{(-1)^{k+j+1}}{2(I-q_0)}\sqrt{(\Omega_k\Omega_j)_0}\,(\hat{c}^\dagger_k + \hat{c}_k)(\hat{c}^\dagger_j + \hat{c}_j). \end{aligned} \tag{B7}$$

Finally, we consider a quadratic potential V and introduce the vibrating mirror ladder operators $\{b, b^\dagger\}$ in a way that $\delta q = x_{\rm zpf}(b + b^\dagger)$, where $x_{\rm zpf}$ is the zero-point-fluctuation amplitude of the vibrating mirror. By reducing all the modes to one ($k = j = 1$), the system Hamiltonian in Eq. (B2) can be written as

$$\begin{aligned}\hat{H} = &\omega_a\hat{a}^\dagger\hat{a} + \omega_b\hat{b}^\dagger\hat{b} + \omega_c\hat{c}^\dagger\hat{c} \\ &+ \frac{x_{\rm zpf}}{2\pi}\left[\omega_c^2(\hat{c} + \hat{c}^\dagger)^2 - \omega_a^2(\hat{a} + \hat{a}^\dagger)^2\right](\hat{b} + \hat{b}^\dagger). \end{aligned} \tag{B8}$$

Defining a coupling strength $g = \omega_c^2\, x_{\rm zpf}/\pi = \omega_c\, x_{\rm zpf}/(I - q_0)$ the Eq. (1) in the main text is obtained. Note that since $\hbar = 1$ the coupling strength g has the right units.

APPENDIX C: EFFECTIVE HAMILTONIAN WITH THE GENERALIZED JAMES' METHOD

For interacting quantum systems that are strongly detuned, an effective Hamiltonian can be derived using the generalized James' effective Hamiltonian method [54]. To apply this method to Eq. (1) in the main text, we first rewrite it in the

interaction picture,

$$\hat{H}_{\rm I}(t) = g\left[\hat{c}^\dagger\hat{c} - \frac{\omega_a^2}{\omega_c^2}\hat{a}^\dagger\hat{a}\right]\hat{b}\,e^{-i\omega_b t} + \frac{g}{2}\left[(\hat{c})^2\hat{b}\,e^{-i(\omega_b+2\omega_c)t} - \frac{\omega_a^2}{\omega_c^2}(\hat{a})^2\hat{b}\,e^{-i(\omega_b+2\omega_a)t}\right]$$
$$+ \frac{g}{2}\left[(\hat{c}^\dagger)^2\hat{b}\,e^{i(2\omega_c-\omega_b)t} - \frac{\omega_a^2}{\omega_c^2}(\hat{a}^\dagger)^2\hat{b}\,e^{i(2\omega_a-\omega_b)t}\right] + \text{H.c.} \tag{C1}$$

This can be rewritten as

$$\hat{H}_{\rm I}(t) = \sum_k [\hat{h}_k e^{-i\omega_k t} + \hat{h}_k^\dagger e^{i\omega_k t}], \tag{C2}$$

where now the ω_k are a combination of the bare transition frequencies. It turns out that a photon-pair hopping mechanism already appears with a second-order generalized James' effective Hamiltonian method [54]. This accounts for calculating

$$\hat{H}_{\rm I}^{(2)}(t) = \sum_{j,k}\frac{1}{\omega_k}[\hat{h}_j\hat{h}_k^\dagger e^{i(\omega_k-\omega_j)t} - \hat{h}_j^\dagger\hat{h}_k e^{i(\omega_j-\omega_k)t}]. \tag{C3}$$

In the rotating-wave approximation, all frequency contributions which are different from zero can be neglected. Since the frequencies ω_k are all different, we only keep the terms in $\hat{H}_{\rm I}^{(2)}(t)$ where the sum of the exponent is zero.

Starting from Eq. (C1) and considering the resonant condition $\omega_a = \omega_c$, only three terms need to be considered,

$$\begin{aligned}
\hat{h}_1 &= \frac{g}{2}(\hat{c}^{\dagger 2} - \hat{a}^{\dagger 2})\hat{b}^\dagger, && \omega_1 = 2\omega_a + \omega_b,\\
\hat{h}_2 &= \frac{g}{2}(\hat{c}^{\dagger 2} - \hat{a}^{\dagger 2})\hat{b}, && \omega_2 = 2\omega_a - \omega_b,\\
\hat{h}_3 &= \frac{g}{2}\big(\{\hat{c},\hat{c}^\dagger\} - \{\hat{a},\hat{a}^\dagger\}\big)\hat{b}^\dagger, && \omega_3 = \omega_b.
\end{aligned} \tag{C4}$$

From the canonical commutation relations it follows that

$$\begin{aligned}
[\hat{h}_1]\hat{h}_1^\dagger =& \frac{g^2}{4}[\hat{a}^2\hat{c}^{\dagger 2} + \hat{a}^{\dagger 2}\hat{c}^2 - \hat{c}^{\dagger 2}\hat{c}^2 - \hat{a}^{\dagger 2}\hat{a}^2 + 2\hat{b}^\dagger\hat{b}(\{\hat{c},\hat{c}^\dagger\} + \{\hat{a},\hat{a}^\dagger\})],\\
[\hat{h}_2]\hat{h}_2^\dagger =& \frac{g^2}{4}[\hat{c}^{\dagger 2}\hat{c}^2 + \hat{a}^{\dagger 2}\hat{a}^2 - \hat{c}^{\dagger 2}\hat{a}^2 - \hat{a}^{\dagger 2}\hat{c}^2 + 2\hat{b}\hat{b}^\dagger(\{\hat{c},\hat{c}^\dagger\} + \{\hat{a},\hat{a}^\dagger\})],\\
[\hat{h}_3]\hat{h}_3^\dagger =& -g^2(\hat{c}^\dagger\hat{c} - \hat{a}^\dagger\hat{a})^2,
\end{aligned} \tag{C5}$$

so James' effective Hamiltonian is

$$\hat{H}_{\rm eff}^{(2)} = \left[\omega_a + \frac{g^2(4\omega_a+\omega_b)}{8\omega_a^2 - 2\omega_b^2}\right](\hat{c}^\dagger\hat{c} + \hat{a}^\dagger\hat{a}) + \frac{g^2\big(3\omega_b^2 - 8\omega_a^2\big)}{\big(8\omega_a^2 - 2\omega_b^2\big)\omega_b}[(\hat{c}^\dagger\hat{c})^2 + (\hat{a}^\dagger\hat{a})^2] + \frac{2g^2}{\omega_b}\hat{a}^\dagger\hat{a}\hat{c}^\dagger\hat{c} + \frac{g^2\hat{\mathbb{1}}}{2\omega_a - \omega_b}$$
$$+ \left[\omega_b + \frac{4g^2\omega_a}{4\omega_a^2 - \omega_b^2}(\hat{c}^\dagger\hat{c} + \hat{a}^\dagger\hat{a} + \hat{\mathbb{1}})\right]\hat{b}^\dagger\hat{b} - \frac{g^2\omega_b}{8\omega_a^2 - 2\omega_b^2}(\hat{a}^2\hat{c}^{\dagger 2} + \hat{a}^{\dagger 2}\hat{c}^2). \tag{C6}$$

All the terms but the last one are energy shifts. The latter is the desired hopping mechanism.

APPENDIX D: MONTE CARLO WAVE FUNCTION APPROACH: QUANTUM TRAJECTORY

Following Refs. [60,61], in order to describe the Monte Carlo wave function (MCWF) approach, we introduce the non-Hermitian Hamiltonian,

$$\hat{\mathcal{H}} = \hat{H} - \frac{i}{2}\sum_m \gamma_m\,\hat{\Gamma}_m^\dagger\hat{\Gamma}_m, \tag{D1}$$

describing the effect of the environment between two quantum jumps. Here, $\hat{H}$ represents the Hamiltonian part of the dynamics, and one can either use the full or the effective Hamiltonian, while $\hat{\Gamma}_m$ are the jump operators. The evolution of a quantum trajectory is thus dictated by a non-Hermitian evolution via $\hat{\mathcal{H}}$ interrupted by random quantum jumps. The algorithm to obtain such a dynamics reads as follows:

(i) $|\psi(t)\rangle$ is the normalized wave function at the initial time t.

(ii) The probability that a quantum jump occurs through the mth dissipative channel in a small amount of time dt is

$$\delta p_m(t) = dt\,\gamma_m\,\langle\psi(t)|\hat{\Gamma}_m^\dagger\hat{\Gamma}_m|\psi(t)\rangle, \tag{D2}$$

such that $\delta p_m(t) \ll 1$.

(iii) One randomly generates a real number $\varepsilon \in [0, 1]$.

(iv) If $\sum_m \delta p_m(t) < \varepsilon$, no quantum jump occurs, and the system evolves as

$$|\psi(t+dt)\rangle = \exp(-i\hat{\mathcal{H}}dt) = \mathbb{1} - idt\hat{\mathcal{H}}|\psi(t)\rangle + \mathcal{O}(dt^2). \tag{D3}$$

(v) Otherwise, if $\sum_m \delta p_m(t) > \varepsilon$, a quantum jump occurs. To decide which channel dissipates, a second random number

ε' is generated, and each quantum jump is selected with probability $\delta p_m(t)/[\sum_n \delta p_n(t)]$. The wave function then becomes

$$|\psi(t+dt)\rangle = \hat{\Gamma}_m|\psi(t)\rangle. \tag{D4}$$

(vi) At this point, independently of whether a quantum jump took place, the wave function $|\psi(t+dt)\rangle$ is renormalized and used for the next step of the time evolution. Any quantum jump corresponds to the projection of the wave function associated with a generalized measurement process (wave-function collapse through a positive operator-valued measure) [62]. Although the results of MCWF recover those of the Lindblad master equation, by averaging over an infinite number of trajectories, noise effects determine the convergence rate.

[1] W. Marshall, C. Simon, R. Penrose, and D. Bouwmeester, Towards Quantum Superpositions of a Mirror, Phys. Rev. Lett. **91**, 130401 (2003).

[2] E. Gavartin, P. Verlot, and T. J. Kippenberg, A hybrid on-chip optomechanical transducer for ultrasensitive force measurements, Nat. Nanotechnol. **7**, 509 (2012).

[3] J. D. Teufel, T. Donner, M. A. Castellanos-Beltran, J. W. Harlow, and K. W. Lehnert, Nanomechanical motion measured with an imprecision below that at the standard quantum limit, Nat. Nanotechnol. **4**, 820 (2009).

[4] A. G. Krause, M. Winger, T. D. Blasius, Q. Lin, and O. Painter, A high-resolution microchip optomechanical accelerometer, Nat. Photonics **6**, 768 (2012).

[5] M. Carlesso and M. Paternostro, Opto-mechanical test of collapse models, in *Do Wave Functions Jump?: Perspectives of the Work of GianCarlo Ghirardi*, edited by V. Allori, A. Bassi, D. Dürr, and N. Zanghi (Springer International Publishing, Cham, 2021), pp. 205–215.

[6] G. Anetsberger, O. Arcizet, Q. P. Unterreithmeier, R. Rivière, A. Schliesser, E. M. Weig, J. P. Kotthaus, and T. J. Kippenberg, Near-field cavity optomechanics with nanomechanical oscillators, Nat. Phys. **5**, 909 (2009).

[7] P. Verlot, A. Tavernarakis, T. Briant, P.-F. Cohadon, and A. Heidmann, Scheme to Probe Optomechanical Correlations between Two Optical Beams Down to the Quantum Level, Phys. Rev. Lett. **102**, 103601 (2009).

[8] S. Barzanjeh, A. Xuereb, S. Gröblacher, M. Paternostro, C. A. Regal, and E. M. Weig, Optomechanics for quantum technologies, Nat. Phys. **18**, 15 (2022).

[9] A. Schliesser, O. Arcizet, R. Rivière, G. Anetsberger, and T. J. Kippenberg, Resolved-sideband cooling and position measurement of a micromechanical oscillator close to the Heisenberg uncertainty limit, Nat. Phys. **5**, 509 (2009).

[10] S. Gröblacher, J. B. Hertzberg, M. R. Vanner, G. D. Cole, S. Gigan, K. C. Schwab, and M. Aspelmeyer, Demonstration of an ultracold micro-optomechanical oscillator in a cryogenic cavity, Nat. Phys. **5**, 485 (2009).

[11] J. D. Teufel, T. Donner, D. Li, J. W. Harlow, M. S. Allman, K. Cicak, A. J. Sirois, J. D. Whittaker, K. W. Lehnert, and R. W. Simmonds, Sideband cooling of micromechanical motion to the quantum ground state, Nature (London) **475**, 359 (2011).

[12] I. Wilson-Rae, N. Nooshi, W. Zwerger, and T. J. Kippenberg, Theory of Ground State Cooling of a Mechanical Oscillator Using Dynamical Backaction, Phys. Rev. Lett. **99**, 093901 (2007).

[13] J. Chan, T. P. M. Alegre, A. H. Safavi-Naeini, J. T. Hill, A. Krause, S. Gröblacher, M. Aspelmeyer, and O. Painter, Laser cooling of a nanomechanical oscillator into its quantum ground state, Nature (London) **478**, 89 (2011).

[14] T. Ojanen and K. Børkje, Ground-state cooling of mechanical motion in the unresolved sideband regime by use of optomechanically induced transparency, Phys. Rev. A **90**, 013824 (2014).

[15] K. Stannigel, P. Komar, S. J. M. Habraken, S. D. Bennett, M. D. Lukin, P. Zoller, and P. Rabl, Optomechanical Quantum Information Processing with Photons and Phonons, Phys. Rev. Lett. **109**, 013603 (2012).

[16] L. Garziano, R. Stassi, V. Macrí, S. Savasta, and O. Di Stefano, Single-step arbitrary control of mechanical quantum states in ultrastrong optomechanics, Phys. Rev. A **91**, 023809 (2015).

[17] P. Meystre, A short walk through quantum optomechanics, Annalen der Physik **525**, 215 (2013).

[18] V. Macrí, L. Garziano, A. Ridolfo, O. Di Stefano, and S. Savasta, Deterministic synthesis of mechanical noon states in ultrastrong optomechanics, Phys. Rev. A **94**, 013817 (2016).

[19] M. Eichenfield, R. Camacho, J. Chan, K. J. Vahala, and O. Painter, A picogram- and nanometre-scale photonic-crystal optomechanical cavity, Nature (London) **459**, 550 (2009).

[20] M. Eichenfield, J. Chan, R. M. Camacho, K. J. Vahala, and O. Painter, Optomechanical crystals, Nature (London) **462**, 78 (2009).

[21] X. Zhang, T. Lin, F. Tian, H. Du, Y. Zou, F. S. Chau, and G. Zhou, Mode competition and hopping in optomechanical nano-oscillators, Appl. Phys. Lett. **112**, 153502 (2018).

[22] D. Chang, A. H. Safavi-Naeini, M. Hafezi, and O. Painter, Slowing and stopping light using an optomechanical crystal array, New J. Phys. **13**, 023003 (2011).

[23] M. Schmidt, M. Ludwig, and F. Marquardt, Optomechanical circuits for nanomechanical continuous variable quantum state processing, New J. Phys. **14**, 125005 (2012).

[24] M. Aspelmeyer, T. J. Kippenberg, and F. Marquardt, Cavity optomechanics, Rev. Mod. Phys. **86**, 1391 (2014).

[25] F. Y. Khalili and S. L. Danilishin, Quantum optomechanics, Prog. Opt. **61**, 113 (2016).

[26] A. D. O'Connell, M. Hofheinz, M. Ansmann, R. C. Bialczak, M. Lenander, E. Lucero, M. Neeley, D. Sank, H. Wang, M. Weides, J. Wenner, J. M. Martinis, and A. N. Cleland, Quantum ground state and single-phonon control of a mechanical resonator, Nature (London) **464**, 697 (2010).

[27] F. Rouxinol, Y. Hao, F. Brito, A. Caldeira, E. Irish, and M. LaHaye, Measurements of nanoresonator-qubit interactions in a hybrid quantum electromechanical system, Nanotechnology **27**, 364003 (2016).

[28] G. T. Moore, Quantum theory of the electromagnetic field in a variable-length one-dimensional cavity, J. Math. Phys. **11**, 2679 (1970).

[29] P. D. Nation, J. R. Johansson, M. P. Blencowe, and F. Nori, Stimulating uncertainty: Amplifying the quantum vacuum with superconducting circuits, Rev. Mod. Phys. **84**, 1 (2012).

[30] J. R. Johansson, G. Johansson, C. M. Wilson, and F. Nori, Dynamical Casimir Effect in a Superconducting Coplanar Waveguide, Phys. Rev. Lett. **103**, 147003 (2009).

[31] J. R. Johansson, G. Johansson, C. M. Wilson, and F. Nori, Dynamical Casimir effect in superconducting microwave circuits, Phys. Rev. A **82**, 052509 (2010).

[32] C. Wilson, G. Johansson, A. Pourkabirian, M. Simoen, J. Johansson, T. Duty, F. Nori, and P. Delsing, Observation of the dynamical Casimir effect in a superconducting circuit, Nature (London) **479**, 376 (2011).

[33] V. Dodonov, Fifty years of the dynamical Casimir effect, Physics **2**, 67 (2020).

[34] V. Macrì, A. Ridolfo, O. Di Stefano, A. F. Kockum, F. Nori, and S. Savasta, Nonperturbative Dynamical Casimir Effect in Optomechanical Systems: Vacuum Casimir-Rabi Splittings, Phys. Rev. X **8**, 011031 (2018).

[35] A. Settineri, V. Macrí, A. Ridolfo, O. Di Stefano, A. F. Kockum, F. Nori, and S. Savasta, Dissipation and thermal noise in hybrid quantum systems in the ultrastrong-coupling regime, Phys. Rev. A **98**, 053834 (2018).

[36] A. Settineri, V. Macrì, L. Garziano, O. Di Stefano, F. Nori, and S. Savasta, Conversion of mechanical noise into correlated photon pairs: Dynamical Casimir effect from an incoherent mechanical drive, Phys. Rev. A **100**, 022501 (2019).

[37] S. Butera and I. Carusotto, Mechanical backreaction effect of the dynamical Casimir emission, Phys. Rev. A **99**, 053815 (2019).

[38] A. Ferreri, H. Pfeifer, F. K. Wilhelm, S. Hofferberth, and D. E. Bruschi, Interplay between optomechanics and the dynamical Casimir effect, Phys. Rev. A **106**, 033502 (2022).

[39] O. Di Stefano, A. Settineri, V. Macrì, A. Ridolfo, R. Stassi, A. F. Kockum, S. Savasta, and F. Nori, Interaction of Mechanical Oscillators Mediated by the Exchange of Virtual Photon Pairs, Phys. Rev. Lett. **122**, 030402 (2019).

[40] S. Butera, Influence functional for two mirrors interacting via radiation pressure, Phys. Rev. D **105**, 016023 (2022).

[41] K. Y. Fong, H.-K. Li, R. Zhao, S. Yang, Y. Wang, and X. Zhang, Phonon heat transfer across a vacuum through quantum fluctuations, Nature (London) **576**, 243 (2019).

[42] T. T. Heikkilä, F. Massel, J. Tuorila, R. Khan, and M. A. Sillanpää, Enhancing Optomechanical Coupling via the Josephson Effect, Phys. Rev. Lett. **112**, 203603 (2014).

[43] J. Pirkkalainen, S. Cho, F. Massel, J. Tuorila, T. Heikkilä, P. Hakonen, and M. Sillanpää, Cavity optomechanics mediated by a quantum two-level system, Nat. Commun. **6**, 6981 (2015).

[44] J. R. Johansson, G. Johansson, and F. Nori, Optomechanical-like coupling between superconducting resonators, Phys. Rev. A **90**, 053833 (2014).

[45] E.-j. Kim, J. R. Johansson, and F. Nori, Circuit analog of quadratic optomechanics, Phys. Rev. A **91**, 033835 (2015).

[46] C. K. Law, Interaction between a moving mirror and radiation pressure: A Hamiltonian formulation, Phys. Rev. A **51**, 2537 (1995).

[47] F. Montalbano, F. Armata, L. Rizzuto, and R. Passante, Spatial correlations of field observables in two half-spaces separated by a movable perfect mirror, Phys. Rev. D **107**, 056007 (2023).

[48] H. K. Cheung and C. K. Law, Nonadiabatic optomechanical Hamiltonian of a moving dielectric membrane in a cavity, Phys. Rev. A **84**, 023812 (2011).

[49] M. Alexanian, Two-photon exchange between two three-level atoms in separate cavities, Phys. Rev. A **83**, 023814 (2011).

[50] Y. L. Dong, S. Q. Zhu, and W. L. You, Quantum-state transmission in a cavity array via two-photon exchange, Phys. Rev. A **85**, 023833 (2012).

[51] S. Cui, B. Grémaud, W. Guo, and G. G. Batrouni, Nonlinear two-photon Rabi-Hubbard model: Superradiance, photon, and photon-pair Bose-Einstein condensates, Phys. Rev. A **102**, 033334 (2020).

[52] A. A. Stepanenko, M. D. Lyubarov, and M. A. Gorlach, Two-photon topological states in the array of qubits caused by the effective photon-photon interaction, in *5th International Conference on Metamaterials and Nanophotonics Metanano 2020*, edited by P. Belov and M. Petrov (AIP, New York, 2020), Vol. 2300, p. 020123.

[53] M. H. Nadiki and M. K. Tavassoly, Photon blockade in a system consisting of two optomechanical cavities via photon hopping, Eur. Phys. J. Plus **136**, 279 (2021).

[54] W. Shao, C. Wu, and X.-L. Feng, Generalized James' effective Hamiltonian method, Phys. Rev. A **95**, 032124 (2017).

[55] F. Minganti, V. Macrì, A. Settineri, S. Savasta, and F. Nori, Dissipative state transfer and Maxwell's demon in single quantum trajectories: Excitation transfer between two noninteracting qubits via unbalanced dissipation rates, Phys. Rev. A **103**, 052201 (2021).

[56] V. Macrì, F. Minganti, A. F. Kockum, A. Ridolfo, S. Savasta, and F. Nori, Revealing higher-order light and matter energy exchanges using quantum trajectories in ultrastrong coupling, Phys. Rev. A **105**, 023720 (2022).

[57] J. Jin, D. Rossini, R. Fazio, M. Leib, and M. J. Hartmann, Photon Solid Phases in Driven Arrays of Nonlinearly Coupled Cavities, Phys. Rev. Lett. **110**, 163605 (2013).

[58] W. Chen and A. A. Clerk, Photon propagation in a one-dimensional optomechanical lattice, Phys. Rev. A **89**, 033854 (2014).

[59] M. Schmidt, S. Kessler, V. Peano, O. Painter, and F. Marquardt, Optomechanical creation of magnetic fields for photons on a lattice, Optica **2**, 635 (2015).

[60] J. Dalibard, Y. Castin, and K. Mølmer, Wave-Function Approach to Dissipative Processes in Quantum Optics, Phys. Rev. Lett. **68**, 580 (1992).

[61] K. Mølmer, Y. Castin, and J. Dalibard, Monte Carlo wave-function method in quantum optics, J. Opt. Soc. Am. B **10**, 524 (1993).

[62] H. Wiseman and G. Milburn, *Quantum Measurement and Control* (Cambridge University Press, Cambridge, 2010).